

## Search for $K^+ \rightarrow \pi^+ \nu \bar{\nu}$ at NA62

---

**Volpe Roberta\* for the NA62 Collaboration<sup>†</sup>**

*Dipartimento di Fisica, Università di Firenze and INFN Firenze*

*E-mail: [roberta.volpe@cern.ch](mailto:roberta.volpe@cern.ch)*

The measurement of  $\text{BR}(K^+ \rightarrow \pi^+ \nu \bar{\nu})$  constitutes a precision test of the Standard Model, given the extremely theoretically clean environment. The NA62 Experiment at CERN SPS has been designed to this purpose. Its commissioning phase is complete and the experiment is taking good quality data. A preliminary exploratory analysis, aimed to assess the detector performance and the sensitivity, has been performed using a small fraction of the 2016 data taking.

*XXV International Workshop on Deep-Inelastic Scattering and Related Subjects*

*3-7 April 2017*

*University of Birmingham, UK*

---

\*Speaker.

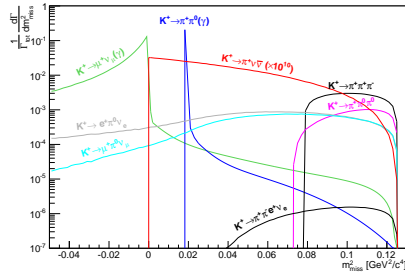
<sup>†</sup>Birmingham, Bratislava, Bristol, Bucharest, CERN, Dubna, Fairfax, Ferrara, Florence, Frascati, Glasgow, Liverpool, Louvain, Mainz, Moscow, Naples, Perugia, Pisa, Prague, Protvino, Rome I, Rome II, San Luis Potosí, Sofia, TRIUMF, Turin, UBC Vancouver.

## 1. The $K^+ \rightarrow \pi^+ \nu \bar{\nu}$ decay

The measurement of  $BR(K^+ \rightarrow \pi^+ \nu \bar{\nu})$  with to a 10% precision is the primary goal of the NA62 experiment at CERN. The great importance to get such a precision arises from the extremely theoretical cleanness of this process environment. The flavor-changing neutral-current decay  $K^+ \rightarrow \pi^+ \nu \bar{\nu}$  has three diagram contributions, two penguin diagrams and one box diagram. The quark-level amplitude is dominated by the top-quark term, with the light-quark contributions being suppressed by the GIM mechanism. Therefore the branching ratio calculation suffers little from hadronic uncertainties. The branching ratio is suppressed in the Standard Model (SM). If computed considering the experimental values and uncertainties on the CKM angles and CPV phase, its value is  $(8.4 \pm 1.0) \times 10^{-11}$ , instead if such SM parameters are taken to be exact, its computed value becomes  $(9.1 \pm 0.7) \times 10^{-11}$  [1]. Many beyond standard model scenarios, which include new sources of flavor violation, predict a large deviation from the above SM values thus making this decay an excellent probe for new physics [2]. The only existent measurement for the  $BR(K^+ \rightarrow \pi^+ \nu \bar{\nu})$  was obtained by the E949 experiment with a result of  $BR(K^+ \rightarrow \pi^+ \nu \bar{\nu}) = 1.73_{-1.05}^{+1.15} \times 10^{-10}$  [3]. A more precise measurement to test the SM is clearly needed. The NA62 measurement has been designed for this task.

## 2. The $BR(K^+ \rightarrow \pi^+ \nu \bar{\nu})$ measurement with NA62 Experiment

The NA62 experiment aims to collect about  $10^{13}$  kaon decays in few years with a kaon beam obtained from the Super Proton Synchrotron (SPS) at CERN. A 400 GeV proton beam, delivering  $10^{12}$  protons per second via SPS, impinges on a 40 cm thick beryllium target. This produces a beam composed of 70%  $\pi^+$  and 23% protons, with  $K^+$  making up only 6% of the beam. The system of collimators and achromat selects 75 GeV positively charged particles with a momentum spread of  $\sigma(p)/p \sim 1\%$  within a polar angle of  $100 \mu\text{rad}$ . The key kinematic variable for the  $BR(K^+ \rightarrow \pi^+ \nu \bar{\nu})$  measurement is the squared missing mass  $m_{miss}^2 = (P_K - P_{\pi^+})^2$ , where  $P_K$  is the 4-momentum of the  $K^+$  and  $P_{\pi^+}$  is the 4-momentum of the charged decay product under the  $\pi^+$  mass hypothesis. The results of the theoretical computation for the main background processes are shown in Fig.1: Fig.1a shows their theoretical shape for the  $m_{miss}^2$  distribution and Fig.1b gives their  $BR$ . In order to get an uncertainty on the measurement comparable to the SM theoretical one at least 100 selected events are needed and the background yield should at most be 20% of the selected events, itself measured with a 10% precision. The signal to background ratio desired can only be obtained if adequate kinematic reconstruction, particle identification, time resolution and hermetic photon/muon vetoes are realized. The NA62 detector was built with these requirements in mind. A schematic layout in the  $xz$  plane is shown in Fig.2 and the main goals of each subdetector are briefly reported in the following. In order to reduce the beam background a kaon identification detector is needed: the KTAG is a Cherenkov counter filled by  $N_2$  with an efficiency greater than 95%, and a time resolution better than 100 ps. The measurements of kaon momentum and direction are performed by a kaon spectrometer, the Gigatracker (GTK). The GTK is composed of three stations, each one made of  $200 \mu\text{m}$  ( $0.5 X_0$ ) thick silicon sensors with a momentum resolution of 0.2% and operates at a 750 MHz rate. The inelastic interactions in the GTK, are detected by a guard ring detector, the CHANTI. The momentum and direction measurements of the charged



(a)

Decay	BR
$K^+ \rightarrow \mu^+ \nu_\mu (\gamma)$	63%
$K^+ \rightarrow \pi^+ \pi^0 (\gamma)$	21%
$K^+ \rightarrow \pi^+ \pi^+ \pi^-$	6%
$K^+ \rightarrow \pi^+ \pi^0 \pi^0$	2%
$K^+ \rightarrow \pi^0 e^+ \nu_e$	5%
$K^+ \rightarrow \pi^0 \mu^+ \nu_\mu$	3%

(b)

Figure 1: (a) Theoretical predictions for the  $m_{miss}^2$  distribution, for the main background and the signal times  $10^{10}$ . (b) BR of the main background kaon decays [4].

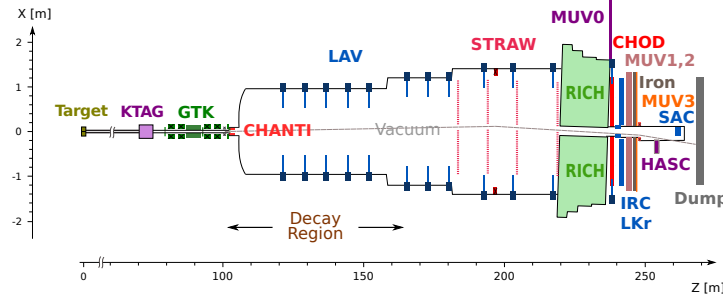


Figure 2: A schematic layout, in the  $xz$  plane, of the NA62 apparatus at SPS [4].

decay products are measured by the STRAW spectrometer, with a relative momentum resolution of  $\sigma_p/p = 0.32\% \oplus 0.008\% p$  (GeV/c). The time of the downstream charged particles is measured by scintillator arrays, the Charged HODoscope (CHOD). One of the main backgrounds is the decay  $K^+ \rightarrow \pi^+ \pi^0$  and requires an hermetic photon veto system composed by the several subdetectors. The Small Angle Calorimeter (SAC) and Inner Ring Calorimeter (IRC) provide an effective photon veto in the angular range  $< 1$  mrad. Both detectors have lead and scintillator plates arranged using Shashlyk configuration. The Liquid Krypton electromagnetic calorimeter (LKr), used in the NA48/2 Experiment, covers the range between 1 and 8.5 mrad. The LKr is a quasi-homogeneous ionization chamber  $26X_0$  deep, that allows measurement of the full electromagnetic shower. Twelve stations of Large Angle Veto (LAV) cover the angular range between 8 and 50 mrad. Stations are made of lead-glass blocks and have an inefficiency  $\sim 10^4$  for photons with  $E > 0.5$  GeV. Another important background is  $K^+ \rightarrow \mu \nu_\mu$  making a muon veto system necessary. Two modules of iron-scintillator sandwiches (MUV1 and MUV2) constitute a hadronic calorimeter which triggers on hadronic deposits and a fast scintillator array (MUV3) identifies and triggers on muons. The identification of the charged secondary particles, pions, muons and positrons, is performed by using the hadronic calorimeters (MUV1 and MUV2), energy deposits in the LKr and the Ring Imaging Cherenkov (RICH) detector. The RICH detector provides a pion identification efficiency of  $\sim 85\%$  for a muon misidentification at most of 1% in the momentum range [15,35] GeV/c. The RICH has a time resolution of better than 100 ps and is used as Level 0 (L0) trigger. The other L0 trigger

conditions applied for the  $K^+ \rightarrow \pi^+ \nu \bar{\nu}$  analysis are signals from the CHOD, LKr, and a veto on signals from MUV3. At level 1 (L1) the KTAG STRAW and LAV (in veto) are used. A L0 *control trigger*, using CHOD signal, has been defined to select control samples. In 2016 the experiment has been completely commissioned and the first set of quality data for the  $K^+ \rightarrow \pi^+ \nu \bar{\nu}$  analysis have been collected. Only  $2.3 \times 10^{10}$   $K^+$  decays in the fiducial region, corresponding to 5% of the quality data collected, have been used to perform a preliminary exploratory analysis. Such an analysis aimed to assess the performances of the detectors and to study the single event sensitivity is described in [5] and summarized in the next section.

### 3. Exploratory analysis on 2016 data

The selection starts with the pion track reconstruction which requires a good-quality positive-charge track reconstructed by the STRAW spectrometer. Such a track should not form a vertex with other tracks and should be in the acceptance of other subdetectors. It also has to be associated to a LKr cluster, a RICH candidate and a CHOD candidate. The time of the CHOD candidate defines the *pion time*. The KTAG candidate which is the closest in time to the pion track identifies the kaon. The time difference and the Closest Distance of Approach between the KTAG and GTK candidates are used to build a discriminant which allows to choose the GTK track. Fig.3 shows the distribution of the pion momentum as a function of the vertex  $z$  for events with both pion and kaon tracks reconstructed and matched, called *kaon* events, and for events where no good kaon track is matched to the pion track called *non-kaon* events. The kaon-decay fiducial region is 60m long and starts 2.5 m downstream from the last GTK station. The distribution of  $m_{miss}^2$  as a function of the

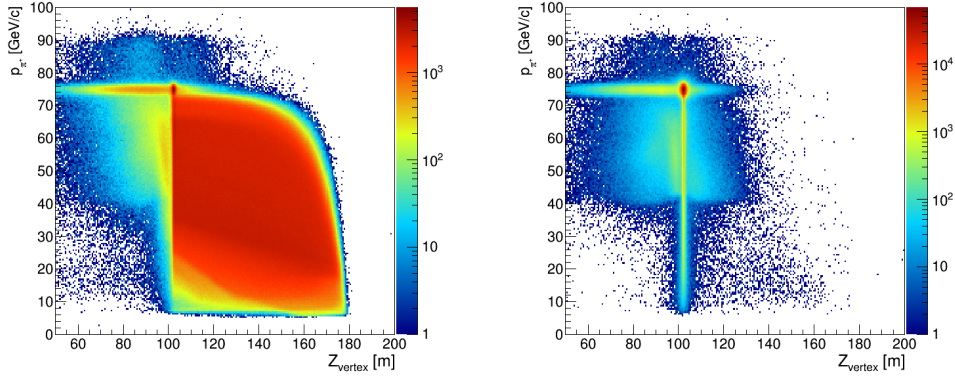


Figure 3:  $\pi^+$  momentum as a function of the vertex  $z$  for kaon events (left) and non-kaon events (right) [5].

pion momentum for events obtained from the control trigger is shown in Fig.4(left). Such a scatter plot is useful to identify different physics processes. The variable  $m_{miss}^2$  can also be obtained in two alternative ways: (i) without the use of the GTK track and using the nominal kaon momentum, referred to as  $m_{miss}^2(\text{NO-GTK})$ ; (ii) without the use of the STRAW track and using the RICH to measure the pion momentum, imposing the nominal pion mass. These two different measurements

give a worse  $m_{miss}^2$  resolution worse than when using all the available information, but they are useful as control measurements. Two signal regions are defined by a cut on the pion momentum,  $15 < p_\pi < 35$  GeV/c, and by the following cuts on  $m_{miss}^2$ :

- Signal Region 1:  $0 < m_{miss}^2, m_{miss}^2(\text{NO-GTK}), m_{miss}^2(\text{RICH}) < 0.01$  GeV<sup>2</sup>/c<sup>4</sup>;
- Signal Region 2:  $0.026 < m_{miss}^2, m_{miss}^2(\text{NO-GTK}), m_{miss}^2(\text{RICH}) < 0.086$  GeV<sup>2</sup>/c<sup>4</sup>;

Calling  $\sigma(m_{miss}^2)$  the resolution of  $m_{miss}^2$ , and using the momentum cut  $15 < p_\pi < 35$  GeV/c, background regions are also defined:

- $\pi^+ \pi^0$  region:  $|m_{miss}^2 - m_{\pi^0}^2| < 3\sigma(m_{miss}^2)$  and  $0.01 < m_{miss}^2(\text{RICH}) < 0.03$  GeV<sup>2</sup>/c<sup>4</sup>;
- $\mu^+ \nu$  region:  $-0.04 < m_{miss}^2 < m_{miss}^2(\mu\nu, \text{max}) + 3\sigma(m_{miss}^2)$  GeV<sup>2</sup>/c<sup>4</sup>,  
where  $m_{miss}^2(\mu\nu, \text{max}) = (m_{\pi^+}^2 - m_{\mu^+}^2)(1 - \frac{p_K}{35\text{GeV}/c})$ ;
- $\pi^+ \pi^+ \pi^-$  region:  $m_{miss}^2 > 4m_{\pi^+}^2 - 3\sigma(m_{miss}^2)$ .

Control samples dominated by the major background processes are defined in what follows. A sample dominated by  $K^+ \rightarrow \pi^+ \pi^0$  is selected by requiring a kaon event and two electromagnetic clusters in the LKr. The  $K^+ \rightarrow \mu^+ \nu$  sample is made of events where the STRAW track is matched in time to a MUV3 candidate, a MIP cluster in LKr and candidates in both MUV1 and MUV2. The  $K^+ \rightarrow \pi^+ \pi^0$  sample is used to estimate the resolution of the  $m_{miss}^2$ ,  $\sigma(m_{miss}^2)$ , which is shown in Fig.4(right) as a function of the pion momentum.  $\sigma(m_{miss}^2)$  is obtained from a fit with two Gaussian distributions to the  $m_{miss}^2$  distribution. Its value,  $\sigma(m_{miss}^2) = 10^3$  GeV<sup>2</sup>/c<sup>4</sup>, is compatible with the design values for the GTK and STRAW resolutions. The signal selection is completed by the parti-

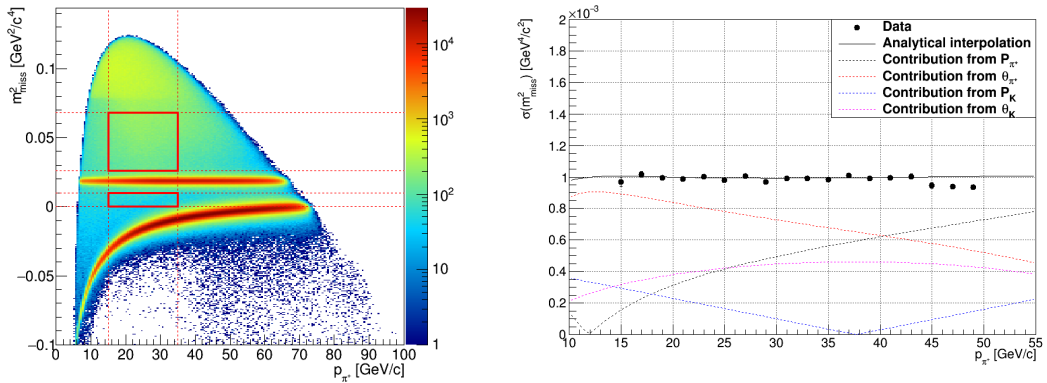


Figure 4: Left: squared missing mass as a function of the selected pion momentum. Right: Resolution of the  $m_{miss}^2$  as a function of the downstream track momentum. Details in [5].

cle ID and the photon rejection. The pion ID as performed by the calorimeters requires no MUV3 candidate matched with the pion track. Furthermore, 13 variables, obtained from information from LKr, MUV1, MUV2 and STRAW candidates, are used to build a Boosted Decision Tree which separates muons from pions. The algorithm which reconstructs the RICH rings, employed in this

analysis, is independent from the STRAW spectrometer measurement. The pion/muon separation power of the calorimeters and RICH has been estimated with the control samples  $K^+ \rightarrow \pi^0 \pi^+$  and  $K^+ \rightarrow \mu^+ \nu$ . Their performances depend on the track momentum; in the [15, 35] GeV/c range, the average value for the pion identification efficiency, combining the RICH and Calorimeter tools, is about 60% for a muon efficiency of  $10^{-7}$ . The  $K^+ \rightarrow \pi^+ \pi^0$  control sample is also used to estimate the  $\gamma$  rejection power, which corresponds to an efficiency for the  $\pi^0$  of  $\epsilon_{\pi^0} = (1.2 \pm 0.2) \times 10^{-7}$ . Additional cuts are needed to reduce the multi-charged background, dominated by the 3 pion events, which gives a further 10% of signal loss. In order to assess the sensitivity of the analysis, a simple counting method has been applied. The control sample  $K^+ \rightarrow \pi^+ \pi^0$  used for normalization, is obtained using the control trigger events and applying the signal selection, with the exception of photon rejection. The number of expected signal events is computed as:

$$N_{\pi\nu\nu} = D^{control} \cdot N_{\pi\pi}^{control} \cdot \frac{BR(K^+ \rightarrow \pi^+ \nu \bar{\nu})}{BR(K^+ \rightarrow \pi^+ \pi^0)} \cdot \frac{A_{\pi\nu\nu}}{A_{\pi\pi}} \cdot \epsilon^{trigger} \quad (3.1)$$

where  $D^{control}$  is the down-scale of the control trigger (400),  $N_{\pi\pi}^{control}$  is the number of  $\pi^+ \pi^0$  events in the control sample,  $A_{\pi\nu\nu}$  and  $A_{\pi\pi}$  are the acceptances of signal and control samples respectively and  $\epsilon^{trigger}$  is the  $K^+ \rightarrow \pi^+ \nu \bar{\nu}$  trigger efficiency.  $A_{\pi\nu\nu}$  and  $A_{\pi\pi}$  have common factors which cancel out in the ratio, and a factor 0.7 is left due to kinematic differences, estimated with MC simulation.  $\epsilon^{trigger}$  is uncorrelated with the selection efficiency and a preliminary conservative data-driven estimation gives 85%. The result obtained for this small dataset is  $N_{\pi\nu\nu}^{exp} = 0.064$ . The numbers of expected background events are summarized in Tab.1. They are obtained by multiplying the number of events in the  $\pi^+ \pi^0$ ,  $\mu^+ \nu$  and  $\pi^+ \pi^- \pi^+$  regions, by the fraction of events in the respective control samples in the signal regions. No events were found in the signal

Process	$f_{SignalRegion}$	Estimation method	$N^{exp}$
$K^+ \rightarrow \pi^+ \pi^0$	$(5.9 \pm 0.2) \times 10^{-4}$	from data	0.024
$K^+ \rightarrow \mu^+ \nu$	$(2.9 \pm 0.2) \times 10^{-4}$	from data	0.011
$K^+ \rightarrow \pi^+ \pi^- \pi^+$	$\sim 10^{-4}$	from MC	0.017
$K^+ \rightarrow \pi^+ \nu \bar{\nu}$			0.064

Table 1: Number of expected events, with 5% of data sample collected in 2016, for the main background events and signal [5].

regions after the full selection. The signal acceptance of this very preliminary analysis is 0.033 which corresponds to a single event sensitivity of about  $10^{-9}$ . Several improvements on the selection and reconstruction algorithms are planned in order to reach a better signal to background ratio and the improved analysis with the full 2016 dataset is in progress.

## References

- [1] A.J. Buras, D. Buttazzo, J. Girrbach-Noe and R. Knegjens, *JHEP* 1511 (2015) 033
- [2] M. Blanke, A.J. Buras and S. Recksiegel, *Eur. Phys. J C* 76 no.4, 182 (2016).
- [3] E949 Collaboration. Artamonov et al., *Phys. Rev. D* 79 (2009) 092004.
- [4] NA62 Collaboration, *JINST* 12 (2017) no.05, P05025.
- [5] NA62 Collaboration, *CERN-SPSC-2017-013*, *SPSC-SR-208*.